DOI: 10.1007/s10856-014-5269-2

J Mater Sci: Mater Med (2014) 25:2297–2303
DOI 10.1007/s10856-014-5269-2

Study of in vitro degradation of brushite cements scaffolds

Caroline de Oliveira Renó · Nicholas C. Pereta · Celso A. Bertran · Mariana Motisuke · Eliandra de Sousa

Received: 16 December 2013 / Accepted: 1 July 2014 / Published online: 17 July 2014

Abstract An interest path to fabricate supports for tissue engineering is to foam calcium phosphate cement's pastes leading to an increase on material's total porosity and interconnectivity which facilitates cells' adhesion, proliferation and differentiation. The aim of this work is to develop scaffolds of brushite cement and to evaluate its in vitro degradation rate. Macroporosity was obtained by foaming the liquid phase with different non-ionic surfactants (Tween 80 and Lutensol ON-110). The foam stability was achieved by adding chitosan. The scaffolds were immersed in Ringers® solution during 7, 14, 21 and 28 days and samples' microstructure, weight loss, mechanical resistance and apparent porosity were evaluated. Both scaffolds presented interconnected macropores with sizes ranging from 100 to 360 μm and total porosities higher than 60 %. These properties could facilitate cell infiltration, bone growth and vascularization. The scaffolds obtained in this work should be considered as promising materials for application in bone tissue engineering.

C. de O. Renó (✉) · N. C. Pereta · M. Motisuke · E. de Sousa
Bioceramics Laboratory - Science and Technology Institute, Federal University of São Paulo (UNIFESP), 330 Talim Street - Vila Nair, São José dos Campos, São Paulo, SP 12231-280, Brazil
e-mail: c.reno@unifesp.br

C. A. Bertran
Physical Chemistry Department, The Institute of Chemistry, University of Campinas (UNICAMP), Campinas, SP, Brazil

1 Introduction

More than two decades ago, calcium phosphate cements (CPCs) were discovered as advanced bioceramics because of their ability to form a moldable paste that self-set in vivo [1–3]. Due to their chemical composition, CPCs present properties as bioactivity, biocompatibility, resorbability and osteoconductivity allowing them to be used for bone treatment [2].

CPCs are hydraulic cements which setting reaction leads to the precipitation of one or more crystalline calcium orthophosphates. Cement's mechanical resistance is a consequence of the entanglement of these crystals [3, 4]. There are different formulations of CPCs; however, all of them lead to apatite or brushite as final product. Like any hydraulic cement, CPCs form plastic pastes that could be molded into any shape like dense blocks and scaffolds [3, 5].

Scaffolds are tridimensional porous structures that allow cells to develop throughout the pores [6–8] and, macroporosity and interconnectivity are key factors for scaffolds' biological, chemical and mechanical performance [6, 7, 9].

Using water soluble and biocompatible surfactants as foaming agents during CPC setting reaction is being reported by Montufar et al. [10–12] as a potential path to produce scaffolds with suitable compressive strength and macroporosity to promote fast bone ingrowth.

Chitosan is usually used to stabilize foams and emulsions due its chemical structure. It is a semi-synthetic polymer—part of its processing occurs at laboratory, but it has a natural matrix—that derives from amino polysaccharides. It is nontoxic, biocompatible, biodegradable, bioactive and has bactericidal effects [13–16].

The aim of this study was to synthesize and characterize scaffolds of brushite cement by foaming the liquid phase

Table 1 CPC nomenclature of each kind of specimen based on its preparation

Samples	Liquid phase				Liquid-to-powder ratio (mL/g)
	$C_6H_8O_7$ (wt.%)	H_3PO_4 (wt%)	Chitosan (wt.%)	Surfactant	
CPC_P	1.54	26.16	0	NO	0.80
CPC_C			0.5	NO	
CPC_L			0.5	LUTENSOL ON110	
CPC_T80			0.5	TWEEN 80	

containing Lutensol ON-110 or Tween 80 as foaming agents and chitosan as foam stabilizer.

2 Materials and methods

2.1 Calcium phosphate cement scaffolds

β-TCP was synthesized by solid state reaction as published elsewhere [17, 18]. The resulting powder was analyzed in triplicate by laser diffraction (Mastersizer 2000; Malvern, UK) and the mean particle size (d(0.5)) was 3.63 ± 0.07 μm.

The liquid phase consisted of an aqueous solution containing 1.5 wt.% of citric acid ($C_6H_8O_7$, Synth, Brazil), 26.2 wt.% phosphoric acid (H_3PO_4, Synth, Brazil), and 0.5 wt.% of chitosan (Sigma Aldrich, Germany). The last one was added to stabilize the foam [16, 19].

CPCs scaffolds were prepared by adding a non-ionic surfactant (0.02 wt.% Lutensol ON 110; Basf, Germany or 0.11 wt.% Tween 80; Synth, Brazil) into the liquid phase, which was stirred (IKA®-WERKE, Germany) for 1 min to obtain the foams. The β-TCP powder was carefully mixed with the foam in a liquid-to-powder ratio (L/P) of 0.80 mL/g and the paste was molded into cylindrical silicone molds (10 × 20 mm). Control samples were prepared without chitosan and/or surfactant and were named CPC_P and CPC_C, respectively. All formulations are described in Table 1.

2.2 CPC scaffolds'in vitro degradation rate

In vitro degradation rate was determined by evaluating samples' weight loss (WL) and compressive strength as a function of time. At least six samples of each formulation were weighed and immersed in Ringers® solution at 36.5 °C during 7, 14, 21 and 28 days. After each period, samples were washed with distilled water, dried at 100 °C during 24 h and then weighed again, with resolution of 0.001 g. The WL was calculated by Equation 1 [20], in which "Wo" is the initial weight of the specimen; and "Wd" is the weight of the dry specimen after the different degradation times. The Ringers® solution was refreshed every 48 h, to avoid significant variations in the pH [8].

$$WL(\%) = [(Wo - Wd)/Wo] \times 100 \quad (1)$$

2.3 Characterization

Compressive strength of the samples was evaluated in a universal testing machine (Instron 5500R) with a crosshead speed of 0.5 mm min^{-1}. At least ten specimens were tested for each formulation.

The morphology of the samples' surface of fracture was analyzed by scanning electron microscopy (SEM, JSM5310, JEOL). The samples were coated with gold (Denton Vacuum—Desk II). The macropores sizes for each formulation were measured by analyzing SEM micrographs using ImageJ software.

Crystalline phases formed after CPC setting and during in vitro degradation rate experiments were analyzed by X-ray diffraction (ŕPert Pro—PANalytical- ŕCelerator, CuKα, Ni filter, 10 a 40° (2θ), 0.02 °/s, 45 kV and 40 mA). JCPDS files used for phase identification were 09-0077 for brushite and 09-0169 for β-TCP.

Semi-quantitative phase analyses were performed on the XRD patterns collected from powdered cement samples by the direct comparison method. This analysis is based on the fact that XRD peaks intensities of a particular phase in a multi-phase sample are proportional to its mass fraction [21].

Samples' total porosity was obtained by Equation 2 [23] in which "d" is the geometrical density of the specimen, and d_{cement} is the cements' theoretical density which was calculated, for each formulation, by Equation (3). $d_{brushite}$ and $d_{[beta]\text{-}TCP}$ are the theoretical density of brushite (2.32 g/cm^3) and β-TCP (3.07 g/cm^3), respectively. $X_{brushite}$ and $X_{[beta]\text{-}TCP}$ are the mass fraction of each phase obtained by the semi-quantitative analysis.

$$P = 1 - (d/d_{cement}) \quad (2)$$

$$d_{cement} = d_{brushite} \times X_{brushite} + d_{[beta]-TCP} \times X_{[beta]-TCP} \quad (3)$$

Xu, et al. (2001) showed that this method is a simple way to calculate total porosity with values closely matched with the measured by mercury intrusion method [22].

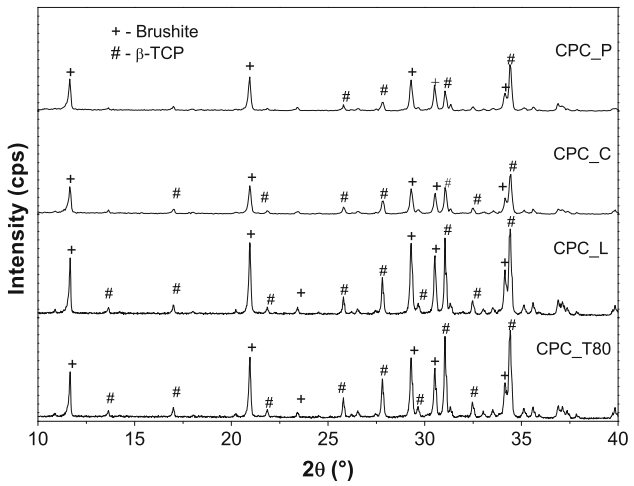

Fig. 1 XRD patterns of as prepared cements and scaffolds samples

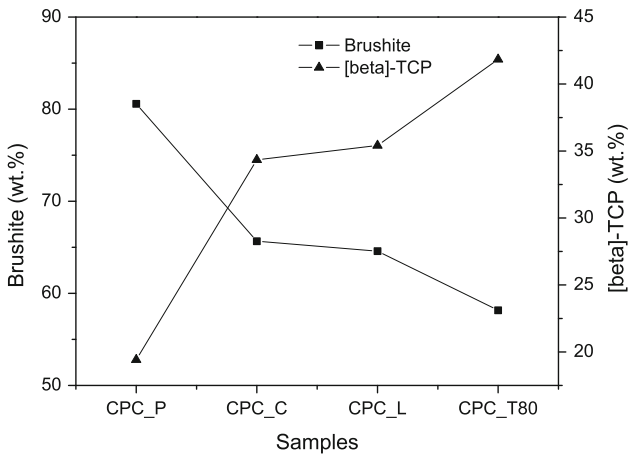

Fig. 2 Mass fraction of each cement and scaffold sample

3 Results and discussion

Scaffolds of CPC were obtained by adding non-ionic surfactants into the liquid phase [10–12]. Chitosan was necessary in order to maintain the stability of the foam and to prevent the collapse of the porous structure during cement setting [16, 19, 24].

Cement setting reaction took place as expected; β-TCP has reacted with H_3PO_4 resulting in brushite ($CaHPO_4{\cdot}2H_2O$) [3] as indicated by the XRD patterns of the as prepared cement and scaffolds specimens (Fig. 1). For all samples, setting reaction was not complete; thus, in the final composition there is a mixture of β-TCP and brushite [3].

Moreover, the foaming process has influenced on β-TCP → brushite conversion once XRD peaks are more intense for foamed samples, CPC_L and CPC_T80. Indeed, as observed on the semi-quantitative analysis of Fig. 2, β-TCP mass fraction for CPC_L and CPC_T80 are higher (36 and 42 wt.%, respectively) when compared with the no foamed samples (19 wt.% for CPC_P and 34 wt.% for CPC_C). This probably occurred because of the difficulty of mixing the powder with the foam, without destroying it and before the initial setting time. The presence of unreacted β-TCP could also be seen in the SEM micrographs (Fig. 3), which is indicated by white arrows.

Figure 4 shows the XRD patterns for CPC_L scaffolds after each period of degradation (7, 14, 21 and 28 days) in Ringers® solution. No different crystalline phases were observed leading to the conclusion that samples' degradation took place by only β-TCP and brushite dissolution in Ringers®. Since brushite is more soluble than β-TCP [25], an inversion on the phases' mass fraction has occurred: after 28 days immersed in Ringers® solution, the sample CPC_L presented 45 wt.% of brushite and 55 wt.% of β-TCP. This behavior was also observed for the others studied compositions.

The microstructure of each sample before and after 28 days of degradation is shown in Fig. 5. It can be observed that sample CPC_P_0d has no macropores and sample CPC_C_0d exhibits a macroporous structure with a small amount of interconnected pores. In contrast, foamed samples, CPC_L and CPC_T80, present a homogeneous distribution of macropores with interconnected pores larger than 50 μm. For both samples, macropores seem to be almost spherical and with diameters varying from 100 to 360 μm. Other authors state that scaffolds with pore diameters ranging from 100 to 800 μm facilitate cell attachment and proliferation [26, 27]. The samples prepared by the foaming process presented pore size distribution between this ideal range.

Samples' total porosities before degradation, calculated using equations 2 and 3,were 49.5 ± 2.6 for CPC_P, 58.6 ± 2.6 for CPC_C, 62.0 ± 2.8 for CPC_L and 65.8 ± 2.8 for CPC_T80. As expected, scaffolds presented higher porosity when compared with the no foamed samples, this also can be observed in Fig. 5. In a previous work our group has employed gelatin as a foaming agent [24] and the total porosity for brushite cement containing 0.5 wt.% of gelatin was 58.7 ± 2.4 %. Thus, comparing both studies, it can be observed that the non-ionic surfactants employed here are more effective to produce samples with higher porosity.

Moreover, it can also be observed in Fig. 5 that all samples had their porosity increased after 28 days of immersion in Ringers® solution due to β-TCP and brushite dissolution.

The weight loss of cements and scaffolds samples as function of time is presented in Fig. 6. With the immersion time prolongation, the weight loss of all samples increased. This effect is more pronounced for CPC_T80 scaffolds, which after 7 days of degradation had the highest weight

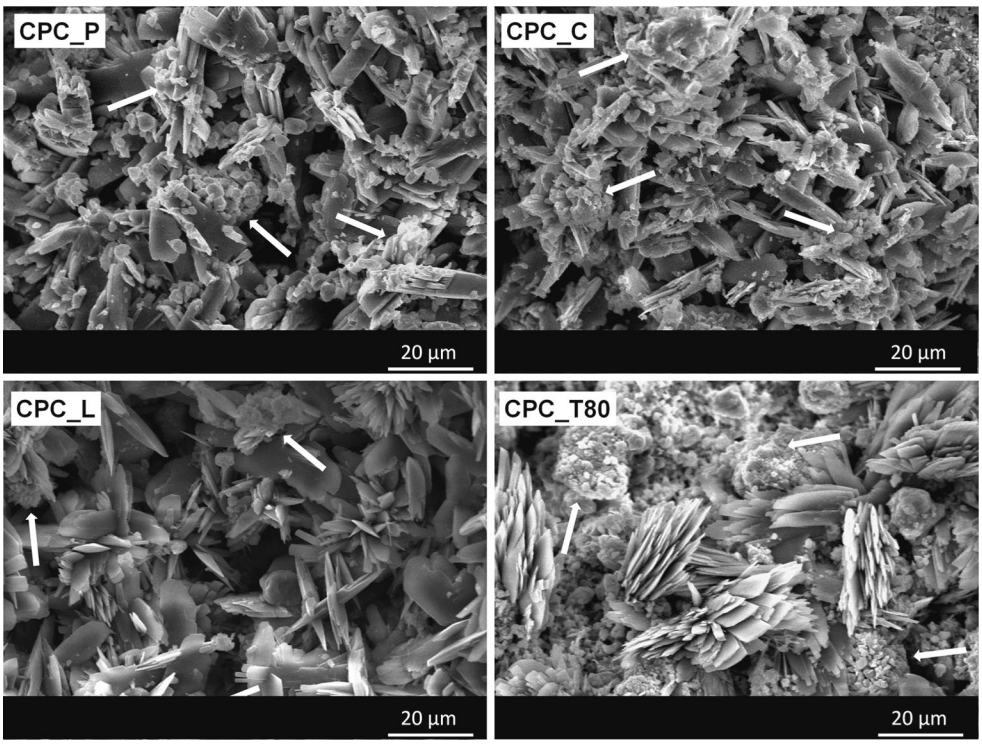

Fig. 3 SEM micrographs of fracture surface for cements and scaffolds samples without degradation. White arrows represents β-TCP

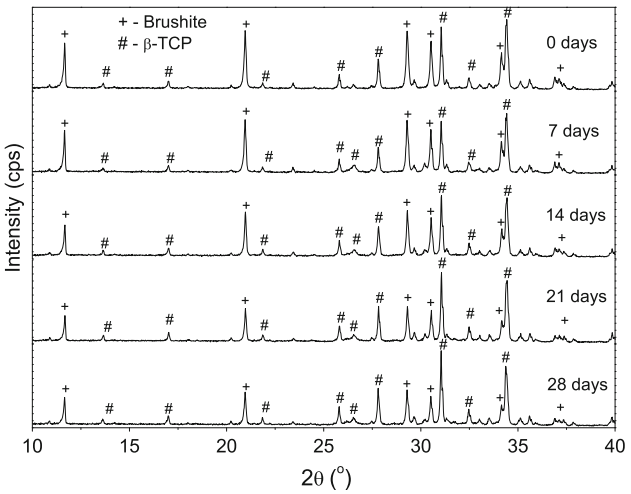

Fig. 4 XRD patterns of CPC_L scaffolds after different degradation periods (0, 7, 14, 21 and 28 days)

loss when compared with the other samples. After 28 days, this sample had 15.8 ± 0.9 % of weight loss while the cements without surfactant, CPC_P and CPC_C, presented 11.2 ± 0.4 and 10.8 ± 0.8 %, respectively. This behavior is due to scaffold's porosity that gives higher surface area to the material, allowing greater contact with Ringers® solution, which leads to higher rates of degradation [8]. Sample CPC_L presented an accentuated weight loss in the first 7 days of degradation. Nevertheless, during the following days it presented a similar behavior to samples CPC_P and CPC_C, with 28 days of degradation CPC_L presented 10.5 ± 0.5 % of weight loss.

Figure 7 shows the compressive strength of cements and scaffolds samples as a function of the different periods of degradation. As expected, in all studied times, the scaffolds (CPC_L and CPC_T80) had lower mechanical resistance values when compared with cements without surfactants (CPC_P and CPC_C). The compressive strength before degradation for the foamed samples, was 1.5 ± 0.5 MPa for CPC_L and 0.7 ± 0.3 MPa for CPC_T80, and after 28 days of immersion this values decreased to 1.2 ± 0.3 MPa for CPC_L and 0.4 ± 0.1 MPa for CPC_T80. Nevertheless, mechanical resistance for CPC_L still has values similar to those of cancellous bone (1–12 MPa) [28].

A comparison between the scaffolds, CPC_L exhibited better values for mechanical strength as compared to CPC_T80 while CPC_T80 presented better values for weight loss. Both properties are important for bone regeneration; however, high degradation rates can promote the bone growth into the scaffold and consequently overcome mechanical resistance loss.

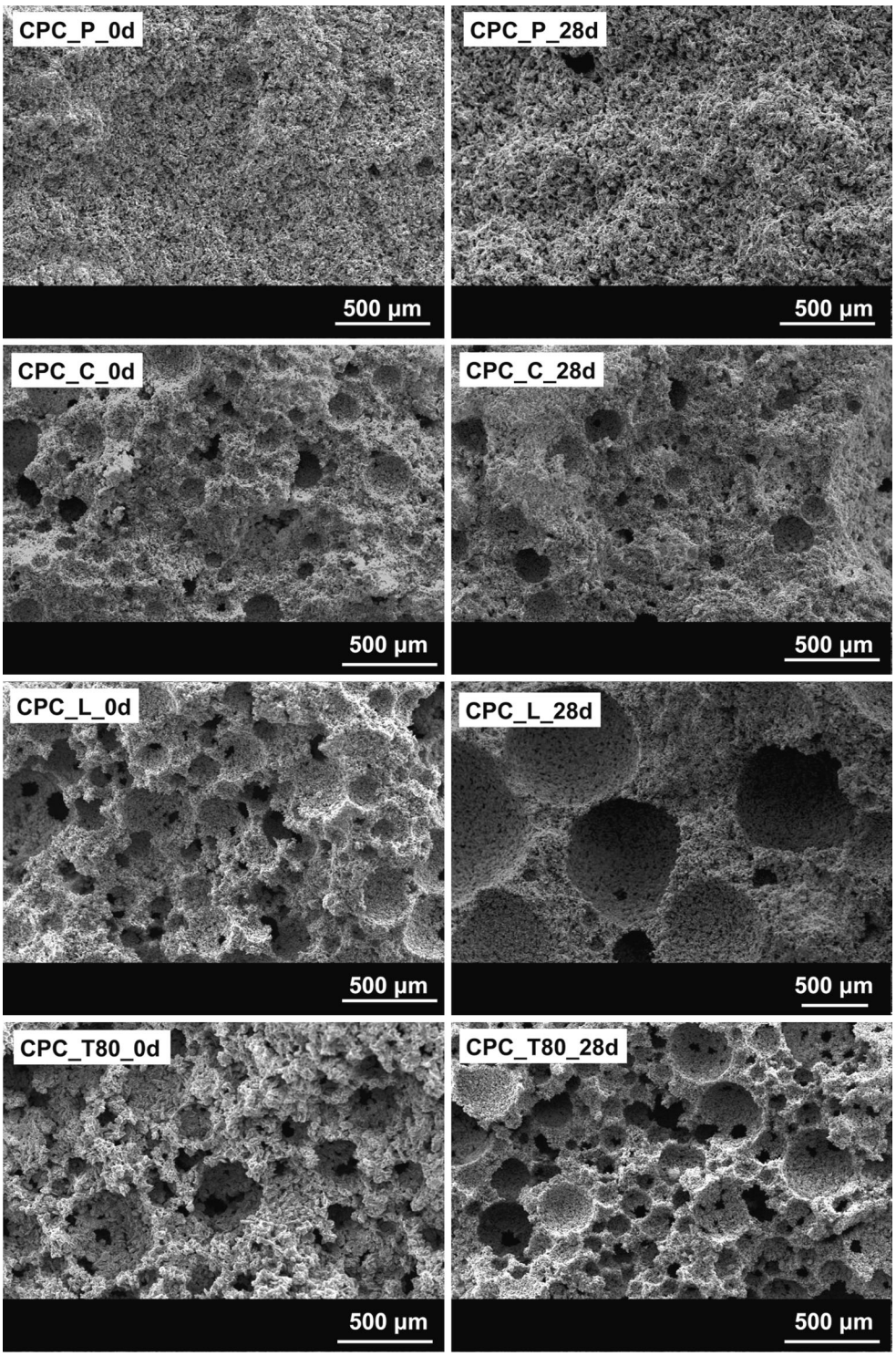

Fig. 5 SEM micrographs of fracture surface for cements and scaffolds samples without degradation (_0d) and with 28 days of degradation (_28d)

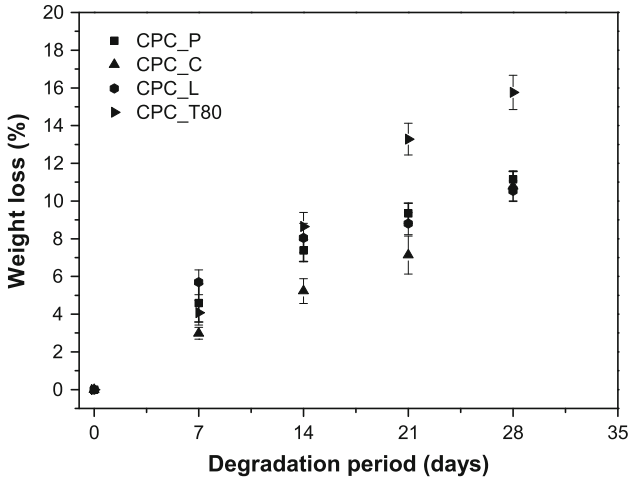

Fig. 6 Weight loss of cements and scaffolds samples as a function of the degradation period (0, 7, 14, 21 and 28 days)

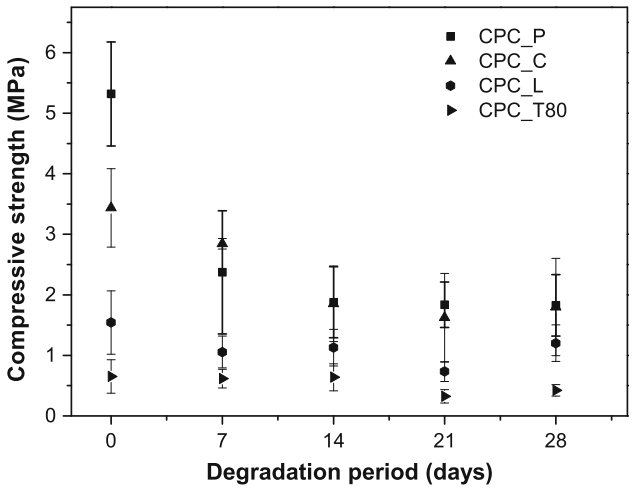

Fig. 7 Compressive strength of cements and scaffolds samples as a function of the degradation period (0, 7, 14, 21 and 28 days)

4 Conclusion

CPC scaffolds were obtained by foaming the cement liquid phase in which non-ionic surfactants were added: Tween 80 or Lutensol ON 110. Both scaffolds presented macropores with sizes ranging from 100 to 360 μm, interconnected pores and higher total porosity when compared with the no foamed samples. As expected, after in vitro degradation, the weight loss has increased in spite of decreasing the compressive strength. Thus, both scaffolds, CPC_L and CPC_T80, should be considered as promising materials for bone treatment.

Acknowledgments The authors would like to thank The São Paulo Research Foundation (FAPESP) for the financial support (Processes Numbers 2012/21198-0, 2010/00863-0 and 2011/09240-9) and João Paulo Barros Machado, PhD from the Laboratory of Sensors and Materials (LAS) of the National Institute of Space Research (INPE) for permitting XRD analysis.

References

1. Van den Vreken NMF, Pieters IY, Declercq HA, Cornelissen MJ, Verbeeck RMH. Characterization of calcium phosphate cements modified by addition of amorphous calcium phosphate. Acta Biomater. 2010;6:617–25.
2. Ginebra M, Espanol M, Montufar E. New processing approaches in calcium phosphate cements and their applications in regenerative medicine. Acta Biomater. 2010;6:2863–73.
3. Ginebra M-P, Canal C, Espanol M, Pastorino D, Montufar EB. Calcium phosphate cements as drug delivery materials. Adv Drug Deliv Rev. 2012;64:1090–110.
4. Espanol M, Perez RA, Montufar EB, Marichal CA, Sacco A, Ginebra MP. Intrinsic porosity of calcium phosphate cements and its significance for drug delivery and tissue engineering applications. Acta Biomater. 2009;5:2752–62.
5. Perez RA, Del Valle S, Altankov G, Ginebra MP. Porous hydroxyapatite and gelatin/hydroxyapatite microspheres obtained by calcium phosphate cement emulsion. J Biomed Mater Res. 2011;97:156–66.
6. Karageorgiou V, Kaplan D. Porosity of 3D biomaterial scaffolds and osteogenesis. Biomaterials. 2005;26:5474–91.
7. Lin CY, Kikuchi N, Hollister SJ. A novel method for biomaterial scaffold internal architecture design to match bone elastic properties with desired porosity. J Biomech. 2004;37:623–36.
8. Feng B, Guolin M, Yuan Y, Changshen L, Zhen W, Jian L. Role of macropore size in the mechanical properties and in vitro degradation of porous calcium phosphate cements. Mater Lett. 2010;64:2028–31.
9. Deville S, Saiz E, Tomsia AP. Freeze casting of hydroxyapatite scaffolds for bone tissue engineering. Biomaterials. 2006;27:5480–9.
10. Montufar E, Traykova T. Comparison of a low molecular weight and a macromolecular surfactant as foaming agents for injectable self setting hydroxyapatite foams: Polysorbate 80 versus gelatine. Mater Sci Eng C. 2011;31:1498–504.
11. Montufar EB, Traykova T, Schacht E, Ambrosio L, Santin M, Planell JA, Ginebra M-P. Self-hardening calcium deficient hydroxyapatite/gelatine foams for bone regeneration. J Mater Sci Mater Med. 2010;21:863–9.
12. Montufar E, Traykova T, Gil C, Harr I. Foamed surfactant solution as a template for self-setting injectable hydroxyapatite scaffolds for bone regeneration. Acta Biomater. 2010;6:876–85.
13. Calero N, Muñoz J, Ramírez P, Guerrero A. Flow behaviour, linear viscoelasticity and surface properties of chitosan aqueous solutions. Food Hydrocoll. 2010;24:659–66.
14. Dash M, Chiellini F, Ottenbrite RM, Chiellini E. Chitosan—A versatile semi-synthetic polymer in biomedical applications. Prog Polym Sci. 2011;36:981–1014.
15. Muzzarelli RAA. Chitins and chitosans for the repair of wounded skin, nerve, cartilage and bone. Carbohydr Polym. 2009;76:167–82.
16. Leffler C, Müller B. Influence of the acid type on the physical and drug liberation properties of chitosan–gelatin sponges. Int J Pharm. 2000;194:229–37.
17. Oliveira AP, Motisuke M, Leal CV, Beppu MM. A Comparative Study between β-TCP Prepared by Solid State Reaction and by Aqueous Solution Precipitation: Application in Cements. Key Eng Mater. 2008;361–363:355–8.
18. Cardoso HAI, Motisuke M, Zavaglia CAC. Análise da influência de dois processos distintos de moagem nas propriedades do pó precursor e do cimento de beta-TCP. Cerâmica. 2012;58:225–8.

19. Hamdine M, Heuzey M-C, Bégin A. Effect of organic and inorganic acids on concentrated chitosan solutions and gels. Int J Biol Macromol. 2005;37:134–42.
20. Qi X, Ye J, Wang Y. Improved injectability and in vitro degradation of a calcium phosphate cement containing poly(lactide-co-glycolide) microspheres. Acta Biomater. 2008;4:1837–45.
21. Cullity BD, Stock SR. Elements of X-Ray diffraction. 3rd ed. Upper Saddle River: Prentice Hall; 2001.
22. Xu HH, Quinn JB, Takagi S, Chow LC, Eichmiller FC. Strong, macroporous, and in situ-setting calcium phosphate cement-layered structures. J Biomed Mater Res. 2001;57:457–66.
23. Xu HHK, Burguera EF, Carey LE. Strong and macroporous calcium phosphate cement: Effects of porosity and fiber reinforcement on mechanical properties. Biomaterials. 2007;28:3786–96.
24. Renó CO, Lima BFAS, de Sousa E, Bertran CA, Motisuke M. Scaffolds of calcium phosphate cement containing chitosan and gelatin. Mater Res. 2013;16:1362–5.
25. Dorozhkin SV. Bioceramics of calcium orthophosphates. Biomaterials. 2010;31:1465–85.
26. Sous M, Bareille R, Rouais F, Cle D, Ame J. Cellular biocompatibility and resistance to compression of macroporous -tricalcium phosphate ceramics. Biomaterials. 1998;19:2147–53.
27. Zhou Y, Xu L, Zhang X, Zhao Y, Wei S, Zhai M. Radiation synthesis of gelatin/CM-chitosan/β-tricalcium phosphate composite scaffold for bone tissue engineering. Mater Sci Eng C. 2012;32:994–1000.
28. Myoui A, Tamai N, Nishikawa M, Hideki Y, Araki N, Nakase T, Akita S, Biomaterials in Orthopedics. Marcel Dekker, Inc.; 2004. p. 287–300.